Isotopic evidence of non-thermalized neutron irradiation in solar-gas-rich meteorites: Possibility of the interaction with solar neutrons and activity from the early Sun

Hiroshi Hidaka[1]* and Shigekazu Yoneda[2]

[1]*Department of Earth and Planetary Systems Science, Hiroshima University*
Higashi-Hiroshima 739-8526, JAPAN

[2]*Department of Science and Engineering, National Museum of Nature and Science*
Tokyo 169-0073, JAPAN

*corresponding author

Abstract

$^{150}Sm/^{149}Sm$ and $^{158}Gd/^{157}Gd$ isotopic shifts in extraterrestrial materials provide evidence of the occurrence of neutron capture reactions caused by the interaction of cosmic rays with the surface of the materials. The Sm and Gd isotopic shifts of chemical leachates from the Kapoeta meteorite, known as a solar-gas-rich meteorite, show a clear neutron capture record corresponding to the neutron fluence up to $9.0x10^{15}$ n cm^{-2}. The intensities of the neutron fluences of two fractions from Kapoeta significantly exceed what is expected from the time for cosmic-ray irradiation during the transit to Earth. Furthermore, the combination of Sm and Gd isotopic shifts, defined as $\varepsilon_{Sm}/\varepsilon_{Gd}$ to understand the neutron energy spectrum, shows a different neutron irradiation environment for certain components of Kapoeta ($\varepsilon_{Sm}/\varepsilon_{Gd}$=1.9 ± 0.5, and 1.9 ± 0.7) from those of other meteorites and lunar samples ($\varepsilon_{Sm}/\varepsilon_{Gd}$=0.4-0.9). The isotopic data of Sm and Gd from Kapoeta suggest the irradiation of non-thermalized neutrons with the energies over 1 eV from the early Sun.

Keywords: cosmic rays exposure; meteorite; neutron capture; samarium; gadolinium

1. Introduction

Because planetary materials have been exposed to cosmic rays, the interactions of cosmic rays with the surface of the materials cause nuclear reactions. The accumulation of the nuclear reactions leads to variations of stable isotopic compositions of some elements and production of radioisotopes in the planetary materials. Therefore, cosmic-ray exposure records of meteorites and lunar surface materials can be characterized by isotopic studies. However, meteorites have often experienced multi-stage irradiation according to their location in space. If the meteorite was buried deeper than a few meters in the parent body, it was shielded from cosmic rays irradiation before erupting from the parent body. After fragmentation of the large body by collisions, the smaller object is then irradiated. In this case, the meteorite is affected mainly from galactic cosmic rays (GCR) consisting of more energetic particles than solar cosmic rays (SCR)

On the other hand, SCR consists mainly of less energetic particles than GCR, so interacts with a very shallow surface layer of the target. Solar particles are implanted to at least micrometers depth (Rao et al., 1991). The contribution of SCR exposure is considered to be observed in some regolith brecciated meteorites like Pesyanoe and Khor Temiki, both aubrites, that contain significant amounts of solar gas component (Marti, 1969; Lorenzetti et al., 2003). This suggests the implantation of solar gas by an ancient solar wind before compaction of the regoliths on their parent asteroidal bodies. Kapoeta is a member of the howardite class of stony meteorites, and is also well known as a solar-gas-rich meteorite (Palma et al., 2002). However, previous studies showed that Kapoeta has experienced a complex exposure history (Caffee and Nishiizumi, 2001).

Isotopic shifts in Sm and Gd caused by neutron capture effects are useful indicators to characterize the interaction of cosmic rays with planetary materials in space, because ^{149}Sm, ^{155}Gd and ^{157}Gd have very large thermal neutron capture cross sections (Eugster et al., 1970; Hidaka et al., 1999). Mass spectrometric measurements of Sm and Gd in planetary samples provide information about neutron capture effects derived from cosmic-ray irradiation. A recent neutron capture study of the Sm and Gd isotopes of Pesyanoe also shows significant variations of neutron fluences in six different phases of a small meteorite fragment, starting with the early irradiation before compaction of the parent body (Hidaka et al., 2006). In this study, Sm and Gd isotopic

analyses of gas-rich brecciated meteorites other than aubrites were performed to find a possible contribution of the irradiation from the early Sun. Furthermore, a parameter from the combination of Sm and Gd isotopic shifts can be used effectively to determine the irradiated neutron data, which allows us to consider the irradiation conditions of target materials in space (Lingenfelter et al., 1972). We will also discuss the possibility of solar neutron irradiation on the Kapoeta meteorite from the systematic isotopic data of Sm and Gd.

2. Experimental methods

2.1. Samples

Two samples of gas-rich meteorites, Northwest Africa 801 (hereafter NWA801; CR2), and Kapoeta (howardite), and two brecciated meteorites, Zag (H3-5) and Cook011 (L3-5), were used in this study.

NWA801 contains a significant amount of solar gas in the similar properties as Pesyanoe and Kapoeta. Cook011 was found on the Nullarbor Plain of Australia. Zag is known to have halite and fluid inclusions showing early aqueous activity in the parent body. Cook011 and Zag show isotopic signatures of regolith brecciated meteorites from noble gas studies and contain significant amounts of solar Ne (Nagao, personal communication). Ar isotopic study shows a difference of exposure ages between gray matrix (H3-4) and light phases (H6) in Zag. The CRE age of 4.3 Ma for the light phase of Zag is interpreted as, while that of 66 Ma for the gray matrix is an additional 2π exposure age as precompaction exposure in the asteroidal regolith (Whitby et al., 2000). Among the meteorite samples used in this study, Zag was previously used for Ba isotopic study (Hidaka et al., 2001). NWA801 and Cook011 were the same as the ones characterized by the noble gas isotopes (Nagao, personal communication).

The Kapoeta meteorite is well known as a highly gas-rich meteorite that experienced early irradiation by cosmic rays, but its irradiation history is complicated and still disputable with regard to evidence for possible contribution of early solar irradiation during the regolith process (Wieler et al., 2000; Caffee and Nishiizumi, 2001). The data of cosmogenic radionuclides suggest that Kapoeta has a 4π exposure age of 3 Ma and a small body with a diameter about 20 cm (Caffee and Nishiizumi, 2001). Kapoeta also shows Sm isotopic evidence of neutron capture effects,

possibly derived from precompaction, although the Sm isotopic shifts from several fragments provided significant variation up to the neutron fluence of $(2.0 \pm 0.4)x10^{15}$ ncm^{-2} (Rajan and Lugmair, 1988).

2.2. Chemical treatments

Each sample weighing 100 to 200 mg, was decomposed by HF + $HClO_4$. After evaporation to dryness, the sample was re-dissolved in 1 mL of 2M HCl. Conventional ion exchange techniques using two-column procedures were carried out to chemically separate Sm and Gd. The first column packed with cation exchange resin (Bio-Rad AG50WX8, 200-400 mesh, H^+ form, 50 mm length, 4.0 mm inner diameter) was used for the separation of the rare earth elements (REE) fraction from the major elements. The second column packed LN resin (Eichrom Tech. Inc., LN-B50-A, particle size 100-150 μm, 100 mm length, 2.5 mm inner diameter) for Sm and Gd separation from other REE (Hidaka and Yoneda, 2007). A Micro-mass VG 54-30 thermal ionization mass spectrometer equipped with seven Faraday cup collectors was used for the isotopic measurements of Sm and Gd (Hidaka et al., 1999). Ion beam intensities of 2.0 to $4.0x10^{-12}$ A for ^{152}Sm and 1.0 to $2.0x10^{-12}$ A for ^{158}Gd were obtained for individual analyses.

Zag consists of light-colored H6 clast and gray H3-4 matrix. In addition to a whole rock sample (Zag #1), 200 mg of clast (Zag #2) and matrix (Zag #3) were individually separated from a main fragment, and used for the Sm and Gd isotopic study.

Because the starting weight of Kapoeta used in this study was limited, the sample was not large enough to perform mineral separation for individual Sm and Gd isotopic measurements. Therefore, a sequential acid-leaching experiment was carried out on the whole rock of Kapoeta, where 200 mg of the powdered sample was leached by 5 mL of 2 M HCl (Kapoeta #2), and aqua regia (Kapoeta #3) in succession. The residue (Kapoeta #4) was finally decomposed by HF + $HClO_4$ with heat. Apart from the acid-leaching treatment, about 100 mg of the powdered sample (Kapoeta #1) was completely decomposed by HF + $HClO_4$ with heat, and used for the whole rock analysis. A part of the fractions obtained by the acid-leaching procedure were used for the determination of REE abundances by inductively coupled plasma mass spectrometry (ICP-MS; VG PlasmaQuad III), because ICP-MS is conveniently applied for trace

element analysis of small quantity samples. The analytical conditions of ICP-MS were previously reported (Shinotsuka et al., 1995).

3. Results and discussion

3.1. Sm and Gd isotopic shifts

The isotopic compositions of Sm and Gd of individual samples are shown in Table 1. An integrated thermal neutron flux provides isotopic shifts of $^{150}Sm/^{149}Sm$ and $^{158}Gd/^{157}Gd$ in some meteorites, because ^{149}Sm and ^{157}Gd have extraordinarily large thermal neutron capture cross sections, 40140 and 254000 barns, respectively. Isotopic shifts of $^{150}Sm/^{149}Sm$ greater than the analytical uncertainties (2σ of the mean) were observed in Kapoeta #2, Kapoeta #3, Zag #1, Zag #2, NWA801 and Cook011. Isotopic shifts of Gd were also observed in the six samples, although the Gd isotopic data always includes larger analytical uncertainties than those of Sm because of low intensities of the ion beam due to very small amounts of Gd dissolved in the leachates. Figure 1 shows correlation diagrams for $^{149}Sm/^{152}Sm$ vs. $^{150}Sm/^{152}Sm$ and $^{157}Gd/^{160}Gd$ vs. $^{158}Gd/^{160}Gd$.

The parameters to characterize neutron capture reactions of individual meteorite samples are listed in Table 2. The isotopic shifts of $^{150}Sm/^{149}Sm$ and $^{158}Gd/^{157}Gd$ were recalculated from the isotopic data shown in Table 1. Macroscopic neutron capture cross section, Σ_{eff} ($cm^2\ g^{-1}$) reveals the total neutron absorbing properties of the target material of given chemical composition (Lingenfelter et al., 1972). The data of CRE ages were cited from previous studies on cosmogenic nuclides (Whitby et al., 2000; Caffee and Nishiizumi, 2001; Nagao, personal communication). Some of the Σ_{eff} and CRE age data are not shown because of lacking the chemical compositions and cosmogenic data, respectively. The neutron fluences, Ψ were estimated from the Sm isotopic data because of better analytical qualities of Sm rather than Gd. $\varepsilon_{Sm}/\varepsilon_{Gd}$ is the ratios of the ^{149}Sm to ^{157}Gd capture rates defined as follows:

$$\frac{\varepsilon_{Sm}}{\varepsilon_{Gd}} = \frac{\dfrac{(^{150}Sm/^{149}Sm)_{sample} - (^{150}Sm/^{149}Sm)_{STD}}{1+(^{150}Sm/^{149}Sm)_{sample}}}{\dfrac{(^{158}Gd/^{157}Gd)_{sample} - (^{158}Gd/^{157}Gd)_{STD}}{1+(^{158}Gd/^{157}Gd)_{sample}}}$$

Interestingly, the neutron fluences of the chemical separates from Kapoeta

(Kapoeta #2, #3 and #4) show a large variation from $<0.21 \times 10^{15}$ ncm^{-2} (detection limit) to $(9.0 \pm 0.6) \times 10^{15}$ ncm^{-2}, although that from the bulk sample (Kapoeta #1) does not show clear evidence of neutron capture over the detection limit ($<0.72 \times 10^{15}$ ncm^{-2}). On the other hand, Rajan and Lugmair (1988) firstly reported ^{150}Sm/^{149}Sm isotopic shifts from several kinds of Kapoeta samples. Their data also show significant variation ($0<\varepsilon_{150Sm}<+4.0$) corresponding to the neutron fluence up to $(2.0 \pm 0.4) \times 10^{15}$ ncm^{-2}. The data suggest the existence of heterogeneous materials having much larger irradiation records than the matrix component. Some eucritic or diogenitic clats which were previously irradiated in the regolith might have migrated in the Kapoeta matrix. Unfortunately, we cannot identify the specific materials having large isotopic shifts on Sm and Gd, but our data from Kapoeta #1 to #4 also suggest the existence of long-irradiated materials in the bulk sample. One could conclude that the first two leaching steps dissolved only very small fraction of the Kapoeta sample.

Zag also shows heterogeneous isotopic shifts on Sm and Gd caused by mixed irradiation records between irradiated and non-irradiated materials. The difference of neutron capture records even in a single fragment is distinctly observed between the gray matrix Zag #2 and the light-colored clast Zag #3, suggesting multistage exposure consisting of simple 4π exposure for the clast, and 4π and additional 2π exposure for the matrix. Whitby et al. (2000) estimated two cosmic ray exposure (CRE) ages of Zag, 66 Ma for the gray matrix and 4 Ma for the light-colored clast from the ratios of cosmogenic ^{38}Ar relative to Ca ($^{38}Ar_c$/Ca). Our Sm and Gd isotopic data from Zag #2 and #3 are consistent with the CRE ages. Considering that Zag is a large meteorite with recovery mass of 175 kg (Grossman, 1999), the pre-atmospheric size might have been large enough for some fragments to shield the 4π irradiation. Isotopic data of Zag #1 can be explained by two-component mixing between gray matrix and clast, considering the smaller isotopic shifts in Sm and Gd observed in Zag #1 relative to those observed in Zag #2.

3.2. Neutron fluences vs. CRE ages

Figure 2 compares the data from thermal neutron fluences from Sm isotopic shifts in this study with CRE ages from noble gas isotopic analyses of previous studies. Although the CRE age of Kapoeta is complicated, it is assumed to be at least 10 Ma from previous studies (Caffee and Nishiizumi, 2001). Considering the difference in

neutron production rate between aubrites and other meteorite species, the upper limit of 4π irradiation duration estimated from Norton County (CRE age=111 Ma, Ψ=1.48x10^{16} n cm^{-2}) is higher than those of other meteorites having high Σ_{eff} (Hidaka et al., 2006). Two data points from Kapoeta #2 and #3 over the upper limit for the 4π irradiation duration in the figure show large excess in addition to the possible irradiation on the meteorite parent body, assuming 4π irradiation duration of 10 Ma for these two samples. Two leachates Kapoeta #2 and #3 show significant neutron capture records, which is consistent with significant regolith exposure ages of some Kapoeta clasts. On the other hand, all of the other data can be explained by 4π and/or 2π irradiation in the meteoroidal body. The neutron fluence data suggest that some components of Kapoeta suffered from experienced pre-irradiation in the regolith before compaction. Assuming that the pre-irradiation in the regolith occurred at depth around 150 g cm^{-2} which provides the highest thermal neutron production rate, at least 80-100 Ma of exposure duration is required to explain the neutron fluence of (7-9)x10^{15} n cm^{-2}. This scenario is consistent with the results of cosmogenic radionuclides from ^{10}Be, ^{26}Al, ^{36}Cl, and ^{53}Mn (Caffee and Nishiizumi, 2001), revealing the existence of some constituents irradiated from an early active Sun.

The production rate of thermal neutrons depends upon the chemical composition of the target material and its depth location in the parent body. In particular, aubrites generally show higher neutron production rates than other meteorite species such as chondrites and howardites, because of the difference in chemical compositions in whole rock samples (Hidaka et al., 1999; 2006). In general, macroscopic neutron capture cross section, Σ_{eff} (cm^2 g^{-1}) is effectively used for characterization of the whole rock sample (Lingenfelter et al., 1972). Σ_{eff} increases with the contents of Fe, Ti and REE. As shown in Table 2, aubrites generally have lower Σ_{eff} values (0.0015 to 0.0023) than Kapoeta (0.0059) and chondrites (0.00699 to 0.00955), mainly because of the different amounts of Fe, Ti and REE.

3.3. Neutron energy spectra

For many nuclides, neutron capture cross sections are inversely proportional to the speed of the neutron around the thermal neutron energy region. On the other hand, the neutron capture cross sections of some nuclides such as ^{149}Sm and ^{157}Gd deviate from this simple relationship. The combination of isotopic shifts between

$^{150}Sm/^{149}Sm$ and $^{158}Gd/^{157}Gd$, defined as the parameter $\varepsilon_{Sm}/\varepsilon_{Gd}$, can be used to understand the neutron energy spectrum (Lingenfelter et al., 1972), because the resonance energy for neutron capture is different between ^{149}Sm (0.0973 eV) and ^{157}Gd (0.0314 eV). The extent of neutron capture reactions also depends upon the chemical composition of the target, and the depth location of the sample in the meteoroid or meteorite parent body. Figure 3 shows a variation of $\varepsilon_{Sm}/\varepsilon_{Gd}$ as a function of Σ_{eff}, which is interpreted to be the result of differences in the neutron energy spectra. For comparison, the data of representative extraterrestrial materials such as lunar regolith, aubrites and chondrites are cited, and also plotted in the same figure.

The Σ_{eff} value for Kapoeta is estimated as 0.0059, mainly from the chemical composition of major elements and REE (Fukuoka et al., 1977). Even considering the differences in Σ_{eff} values among the samples in this study, $\varepsilon_{Sm}/\varepsilon_{Gd}$ values of Kapoeta #2 (1.9 ± 0.7) and #3 (1.9 ± 0.5) are higher than the others. The data suggest that Kapoeta #2 and #3 were irradiated by higher energy neutrons relative to thermalized neutrons. In most cases, neutron capture reactions near the surface of planetary materials have occurred by thermalized neutrons produced from the interaction of GCR with the planetary materials. In particular, lunar regoliths and aubrites provide clear records of thermal neutron irradiation because of long GCR irradiation under 2π condition.

Calculated neutron fluences of the lunar regoliths from the Apollo 15, 16 and 17 landing sites suggest the irradiation history covering more than 1000 Ma corresponding to the neutron fluences of 1.9 to 9.0×10^{16} n cm^{-2} (Russ et al., 1972; Russ, 1973; Curtis and Wasserburg, 1975; Hidaka et al., 2000; Hidaka and Yoneda; 2007). The variation of the neutron fluences of lunar regoliths has a relationship with their depths, which can be used to discuss the depositional history of the lunar regolith. On the other hand, aubrites have long CRE ages such as Norton County (111 Ma) and Mayo Belwa (117Ma), and their neutron fluences are high up to 4×10^{16} n cm^{-2}, as shown in Cumberland Falls. Considering the poor correlation between the CRE ages and estimated neutron fluences of aubrites (Hidaka et al., 1999; 2006), aubrites might have experienced multistep irradiation, possibly with first-stage irradiations near the surface of the parent body (2π exposure), and then space (4π) exposure after ejection from the parent body. Both lunar regoliths and aubrites are considered to have experienced high fluences of thermalized neutrons produced from the interactions with GCR. Pesyanoe is an exceptional case: it contains a large amount of solar gas component (Marti, 1969),

and its high and heterogeneous Sm and Gd isotopic compositions, indicating variations in neutron fluences (2.1 to 2.8x10^{16} n cm^{-2}) even in a fragment a few centimeters in size suggests the early irradiation record during the regolith process of Pesyanoe before compaction (Hidaka et al., 2006). However, the low $\varepsilon_{Sm}/\varepsilon_{Gd}$ values (0.37 to 0.51) of Pesyanoe suggest irradiation by thermalized neutrons. The $\varepsilon_{Sm}/\varepsilon_{Gd}$ values of lunar regoliths range from 0.61 to 0.89 (Russ et al., 1972; Curtis and Wasserburg, 1975; Hidaka and Yoneda, 2007). The $\varepsilon_{Sm}/\varepsilon_{Gd}$ variation observed in a series of lunar samples depends mainly upon their chemical compositions. On the other hand, aubrites generally show lower $\varepsilon_{Sm}/\varepsilon_{Gd}$ values (0.4-0.5) than those of lunar regoliths (Hidaka et al., 1999; 2006). Considering the neutron energy spectra from the difference of the chemical compositions (Σ_{eff}), the difference of $\varepsilon_{Sm}/\varepsilon_{Gd}$ values is reasonable, even from the similar neutron interactions produced from GCR irradiation. Since the prediction by Lingenfelter et al. (1972) supported information on the neutron energies up to at least 1 eV, we cannot simply estimate the neutron energies shown in Kapoeta #2 and #3 simply from the $\varepsilon_{Sm}/\varepsilon_{Gd}$ values. However, very high $\varepsilon_{Sm}/\varepsilon_{Gd}$ values of Kapoeta #2 (1.9 ± 0.7) and #3 (1.9 ± 0.5) cannot be explained only from the interaction by GCR-induced neutrons as far as we know through the Sm and Gd isotopic studies of extraterrestrial materials (Hidaka et al., 1999; 2000: 2006; Hidaka and Yoneda, 2007). Neutron capture reactions caused by non-thermalized neutrons may be required to explain the high $\varepsilon_{Sm}/\varepsilon_{Gd}$ values of Kapoeta #2 and #3.

NWA801 also shows a high $\varepsilon_{Sm}/\varepsilon_{Gd}$ value (1.2 ± 0.4). However, its level is not clear enough to assess the interaction with high-energy neutrons because of the large analytical uncertainty. The parameter $\varepsilon_{Sm}/\varepsilon_{Gd}$ varies not only with neutron energy (temperature) but also with the chemical composition of the target (Σ_{eff}). The model by Lingenfelter, Canfield and Hampel (1972), hereafter LCH model, predicts that $\varepsilon_{Sm}/\varepsilon_{Gd}$ values increase with Σ_{eff}. In our previous study, the regolith samples from the Apollo 17 landing site, having similar Σ_{eff} values (0.009 to 0.0095) with that of NWA801, show $\varepsilon_{Sm}/\varepsilon_{Gd}$ of 0.74-0.82 (Hidaka and Yoneda, 2007). Considering the Σ_{eff} value (0.00955) and the large analytical uncertainty for NWA801, the $\varepsilon_{Sm}/\varepsilon_{Gd}$ value of NWA801 is consistent with capture effects by thermalized neutrons.

The chemical composition data have shown that howardites consist of a mixture of eucrites and diogenites in different proportions except for siderophile elements (Fukuoka et al., 1977; Sisodia et al., 2001). In particular, linear regression

analysis is effective in reconstructing the REE pattern of the Kapoeta whole rock from a mixture of Haraiya (eucrite) and Johnstown (diogenite). Chondrite-normalized REE patterns of acid-leaching fractions from Kapoeta are shown in Figure 4. The results show that the REE pattern of the acid residue (Kapoeta #4) with depletion of lighter REE and a negative Eu anomaly, is similar to those of typical diogenites such as Johnstown, Ibbenbüren and Shalka. On the other hand, the acid leachates (Kapoeta #2 and #3) found with high $\varepsilon_{Sm}/\varepsilon_{Gd}$ values show divergent REE patterns from those of the acid residue. The fraction of Kapoeta #2 shows more flat REE patterns than that of the acid residue, although the heavier REE slightly resembles that of the acid residue (Kapoeta #4). The REE pattern of Kapoeta #3 having a positive Eu anomaly is similar to those of cumulative eucrites such as Moore County and Serra de Mage (Consolmagno and Drake, 1977), although the REE abundance is low because of dilution by other components. It is reasonable to find isotopic evidence for neutron capture effects possibly caused by solar neutrons from the acid-leached phases, because SCR particles have less energy than GCR.

Solar neutrons are produced by the interaction of accelerated ions with the solar atmosphere. Recent observation shows that high-energy solar neutrons induced by the solar flare events could be detected even on the earth (Debrunner et al., 1993; Watanabe et al., 2003; Sako et al., 2006). Neutral particles released from the Sun are not affected by any magnetic fields. Therefore, solar neutrons might have effectively interacted with the meteorite parent body, in particular, during the regolith period, although the survival probability of decay should be considered for neutrons of nonrelativistic energy.

It is unlikely that the high-energy neutron with energies > 1 MeV cause significant shifts in the Sm and Gd isotopic compositions, because the neutron-capture cross sections for these high-energy neutrons are extremely low. On the other hand, low-energy neutrons with energies <1 KeV have higher neutron capture cross sections of ^{149}Sm and ^{157}Gd, but they are unlikely to reach the asteroid belt. Although the solar neutrons with high energies are not directly interactive with Sm and Gd isotopes, they might have lost the energies in inelastic collisions with heavy nuclei in the target materials. Then, the neutrons might have gradually decreased the energies which are sufficiently interactive with ^{149}Sm and ^{157}Gd isotopes. Slowing down of neutrons by collision with the target materials is possible to produce epi-thermal neutrons and high

$\varepsilon_{Sm}/\varepsilon_{Gd}$ in the meteorite.

As another possibility to explain the high $\varepsilon_{Sm}/\varepsilon_{Gd}$ values, GCR irradiation onto a small meteorite with a diameter less than 50 g cm^{-2} dominantly produce high energy neutrons (10^3-10^6 eV) over the energy range of thermal and epi-thermal neutrons (Spergel et al., 1986). Considering a 4π exposure age of 3 Ma for Kapoeta with a small body with a diameter about 20 cm suggested by cosmogenic radionuclides (Caffee and Nishiizumi, 2001), the exposure condition of Kapoeta is sufficient to produce neutrons with energies over 1 eV. However, 4π exposure age of 3 Ma is too short to produce $^{150}Sm/^{149}Sm$ isotopic shifts corresponding to the neutron fluences of (7.0-9.0)x10^{15} ncm^{-2} observed in two leachates. It is reasonable to consider the pre-irradiation in the regolith mainly to explain the significant neutron capture records.

4. Conclusions

Because howardites are considered to be fragments from the regolith of the parent body, it may be reasonable to identify the irradiation effect during the regolith process in some specific phases in the sample. Neutron energy information given by $\varepsilon_{Sm}/\varepsilon_{Gd}$ in two acid-leachates of Kapoeta shows a clear difference from other extraterrestrial materials studied previously (Hidaka et al., 1999; 2000; 2006; Hidaka and Yoneda, 2007). High $\varepsilon_{Sm}/\varepsilon_{Gd}$ values of the Kapoeta leachates are due to the low isotopic shifts in Gd which have large analytical uncertainties. The results reveal that the neutrons acting on some parts of Kapoeta were not as well thermalized as those acting on the other materials. Irradiation of non-thermalized neutrons with the energies probably over 1 eV is a possibility to explain the higher $\varepsilon_{Sm}/\varepsilon_{Gd}$ of some parts of Kapoeta. In general, GCR irradiation produces secondary neutrons which are eventually slowed down to thermal energies, reaching a maximum flux at a depth around 150 gcm^{-2} in the target. Another probable neutron source is the Sun. Considering that the studied meteorite samples contain large amounts of gas components released from the Sun, it is reasonable to detect non-thermalized neutrons from the Sun from the Sm and Gd isotopic shifts caused by neutron capture reactions.

Acknowledgements

We thank Prof. K. Nagao (University of Tokyo) for donating NWA801 and Cook011 samples. Critical comments and suggestions by two anonymous journal

reviewers and the Editor, Dr. R. Carlson were very useful to improve the first draft of the paper. This study was financially supported by a Grant-in-Aid for Scientific Research of Japan Society for the Promotion of Science (to H.H., Nos. 17204051 and 21244086).

References

Caffee, M.W., Nishiizumi, K., 2001. Exposure history of separated phases from the Kapoeta meteorite. Meteorit. Planet. Sci. 36, 429-437.

Consolmagno, G.J., Drake, M., 1977. Composition and evolution of the eucrite parent body: evidence from rare earth elements. Geochim. Cosmochim. Acta 41, 1271-1282.

Curtis, D., Wasserburg, G.J., 1975. Apollo 17 neutron stratigraphy: sedimentation and mixing in the lunar regolith. The Moon 13, 185-227.

Debrunner, H., Lockwood, J.A., Ryan, J.M., 1993. Solar neutron and proton production during the 1990 May 24 cosmic-ray flare increases. Astrophys. J. 409, 822-829.

Eugster, O., Tera, F., Burnett, D.S., Wasserburg, G.J., 1970. Isotopic composition of gadolinium and neutron-capture effects in some meteorites. J. Geophys. Res. 75, 2753-2768.

Fukuoka, T., Boynton, W.V., Ma, M.-S., Schmitt, R.A., 1977. Genesis of howardites, diogenites, and eucrites. Proc. Lunar Sci. Conf. 8, 187-210.

Grossman, J.N., 1999. The Meteoritical Bulletin, No.83, 1999 July. Meteorit. Planet. Sci. 34, A169-A186.

Hidaka, H., Yoneda, S., 2007. Sm and Gd isotopic shifts of Apollo 16 and 17 drill stem samples and their implications for regolith history. Geochim. Cosmochim. Acta 71, 1074-1086.

Hidaka, H., Ebihara, M., Yoneda, S., 1999. High fluences of neutrons determined from Sm and Gd isotopic compositions in aubrites. Earth Planet. Sci. Lett. 173, 41-51.

Hidaka, H., Ebihara, M., Yoneda, S., 2000. Neutron capture effects on samarium, europium, and gadolinium in Apollo 15 deep drill-core samples. Meteor. Planet. Sci. 35, 581 –589.

Hidaka, H., Yoneda, S., Marti, K., 2006. Regolith history of the aubritic meteorite parent body revealed by neutron capture effects on Sm and Gd isotopes. Geochim. Cosmochim. Acta 70, 3449-3456.

Lingenfelter, R.E., Canfield, E.H., Hampel, V.E., 1972. The lunar neutron flux revisited. Earth Planet. Sci. Lett. 16, 355-369.

Lorenzetti, S., Eugster, O., Busemann, H., Marti, K., Burbine, T.H., McCoy, T., 2003. History and origin of aubrites. Geochim. Cosmochim. Acta 67, 557-571.

Marti, K., 1969. Solar-type xenon: a new isotopic compositions of xenon in the Pesyanoe meteorite. Science 166, 1263-1265.

Palma, P.L., Becker, R.H., Pepin, R.O., Schlutter, D.J., 2002. Irradiation records in regolith materials, II: Solar wind and solar energetic particle components in helium, neon, and argon extracted from single lunar mineral grains and from the Kapoeta howardite by stepwise pulse heating. Geochim. Cosmochim. Acta 66, 2929-2958.

Rajan, R.S., Lugmair, G.W., 1988. Solar flare tracks and neutron capture effects in gas-rich meteorite. Lunar Planet. Sci. Conf. XIX, 964-965.

Rao, M.N., Garrison, D.H., Bogard, D.D., Badhwar, G., Murali, A.V., 1991. Comparison of solar flare noble gases preserved in meteorite parent body regolith. J. Geophys. Res. 96, (A11) 19321-19330.

Rao, M.N., Garrison, D.H., Palma, R.A., Bogard, D.D., 1997. Energetic proton irradiation history of the howardite parent body regolith and implications for ancient solar activity. Meteorit. Planet. Sci. 32, 531-543.

Russ, G.P., Burnett, D.S., Wasserburg, G.J., 1972. Lunar neutron stratigraphy. Earth Planet. Sci. Lett. 15, 172-186.

Russ, G.P., 1973. Apollo 16 neutron stratigraphy. Earth Planet. Sci. Lett. 17, 275-289.

Sako, T., Watanabe, K., Muraki, Y., Matsubara, Tsujihara, H., Yamashita, M., Sakai, T., Shibata, S., Valdes-Galicia, J.F., Gonzalez, L.X., Hurtado, A., Musalem, O., Miranda, P., Martinic, N., Ticona, R., Velarde, A., Kakimoto, F., Ogio, S., Tsunesada, Y., Tokuno, H., Tanaka, Y.T., Yoshikawa, I., Terasawa, T., Saito, Y., Mukai, T., Gros, M., 2006. Long-lived solar neutron emission in comparison with electron-produced radiation in the 2005 September 7 solar flare. Astrophys. J. 651, L69-L72.

Shinotsuka, K., Hidaka, H., Ebihara, M., 1995. Detailed abundances of rare earth elements, thorium and uranium in chondritic meteorites: an ICP-MS study. Meteoritics 30, 694-699.

Sisodia, M.S., Shukla, A.D., Suthar, K.M., Mahajan, R.R., Murty, S.V.S., Shukla, P.N., Bhandari, N., Natarajan, R., 2001. The Lohawat howardite: Minealogy, chemistry and cosmogenic effects. Meteorit. Planet. Sci. 36, 1457-1466.

Spergel, M.S., Reedy, R.C., Lazareth, O.W., Levy, P.W., Slatest, L.A., 1986.

Cosmogenic neutron-capture-produced nuclides in stony meteorites. J. Geophys. Res. 91, D483-D494.

Watanabe, K., Muraki, Y., Matsubara, Y., Murakami, K., Sako, T., Tsuchiya, H., Masuda, S., Yoshimori, M., Ohmori, N., Miranda, P., Martinic, N., Ticona, R., Velarde, A., Kakimoto, F., Ogio, S., Tsunesada, Y., Tokuno, H., Shirasaki, Y., 2003. Solar neutron event in association with a large solar flare on 2000 November 24. Astrophys. J. 592, 590-596.

Whitby, J., Burgess, R., Turner, G., Gilmour, J., Bridges, J., 2000. Extinct ^{129}I in halite from a primitive meteorite: Evidence for evaporite formation in the early solar system. Science 288, 1819-1821.

Wieler, R., Pedroni, A., Leya, I., 2000. Cosmogenic neon in mineral separates from Kapoeta: No evidence for an irradiation of its parent body regolith by an early active Sun. Meteorit. Planet. Sci. 35, 251-257.

Table 1

(a) Isotopic composition of Sm

sample	$^{148}Sm/^{152}Sm$	$^{149}Sm/^{152}Sm$	$^{150}Sm/^{152}Sm$	$^{154}Sm/^{152}Sm$
STD1	0.420461	0.516868	0.275996	0.850854
	± 5	± 5	± 2	± 7
STD1	0.420450	0.516720	0.276140	0.850825
	± 2	± 2	± 2	± 4
Kapoeta#1	0.420458	0.516859	0.276008	0.850842
(bulk)	± 30	± 29	± 22	± 45
Kapoeta#2	0.420455	0.516667	0.276190	0.850898
(2M HCl)	± 5	± 5	± 3	± 8
Kapoeta#3	0.420441	0.516613	0.276246	0.850860
(aqua regia)	± 23	± 19	± 19	± 36
Kapoeta#4	0.420463	0.516862	0.276005	0.850860
(acid residue)	± 8	± 8	± 6	± 14
Zag#1	0.420450	0.516844	0.276015	0.850898
(bulk)	± 17	± 12	± 9	± 15
Zag#2	0.420450	0.516828	0.276030	0.850835
(gray matrix)	± 17	± 20	± 16	± 26
Zag#3	0.420473	0.516859	0.275994	0.850830
(clast)	± 20	± 20	± 17	± 15
NWA801	0.420434	0.516791	0.276090	0.850851
(bulk)	± 19	± 15	± 10	± 30
Cook011	0.420451	0.516832	0.276034	0.850853
(bulk)	± 9	± 10	± 8	± 23

All standard errors of the last digits indicated are 2σ of the mean.

STD1 is a non-irradiated standard material (Ψ=0 n cm^{-2}).

STD2 is a neutron-irradiated standard material (Ψ=5.94x10^{15} n cm^{-2}).

(b) Isotopic composition of Gd

sample	$^{154}Gd/^{160}Gd$	$^{155}Gd/^{160}Gd$	$^{157}Gd/^{160}Gd$	$^{158}Gd/^{160}Gd$
STD	0.099750	0.676883	0.715867	1.135845
	± 1	± 5	± 4	± 5
Kapoeta#1	0.099788	0.676842	0.715860	1.135842
(bulk)	± 39	± 41	± 54	± 53
Kapoeta#2	0.099765	0.676828	0.715729	1.135989
(2M HCl)	± 52	± 67	± 58	± 88
Kapoeta#3	0.099766	0.676820	0.715688	1.136039
(aqua regia)	± 75	± 88	± 58	± 76
Kapoeta#4	0.099782	0.676880	0.715847	1.135830
(acid residue)	± 37	± 51	± 42	± 58
Zag#1	0.099756	0.676820	0.715821	1.135891
(bulk)	± 44	± 48	± 34	± 38
Zag#2	0.099778	0.676806	0.715812	1.135906
(gray matrix)	± 36	± 29	± 23	± 33
Zag#3	0.099772	0.676842	0.715877	1.135842
(clast)	± 37	± 55	± 43	± 60
NWA801	0.099744	0.676812	0.715767	1.135954
(bulk)	± 40	± 46	± 39	± 48
Cook011	0.099756	0.676836	0.715803	1.135911
(bulk)	± 32	± 20	± 31	± 45

All standard errors of the last digits indicated are 2σ of the mean.

Table 2 Sm and Gd isotopic shifts and parameters to characterize neutron capture reactions

sample	$^{150}Sm/^{149}Sm$	$^{158}Gd/^{157}Gd$	Σeff ($cm^2\ g^{-1}$)	CRE age (Ma)	Ψ ($x10^{15}$ n cm^{-2})	$\varepsilon_{Sm}/\varepsilon_{Gd}$
STD1	0.533977 ± 6	1.58667 ± 1				
Kapoeta#1 (bulk)	0.534010 ± 52	1.58668 ± 14	0.00590	~10	<0.72	Not determined
Kapoeta#2 (2M HCl)	0.534561 ± 8	1.58718 ± 18			7.0 ± 0.2	1.9 ± 0.7
Kapoeta#3 (aqua regia)	0.534725 ± 42	1.58734 ± 17			9.0 ± 0.6	1.9 ± 0.5
Kapoeta#4 (acid residue)	0.534001 ± 14	1.58669 ± 12			<0.21	Not determined
Zag#1 (bulk)	0.534039 ± 21	1.58684 ± 9	0.00854		0.76 ± 0.31	0.62 ± 0.38
Zag#2 (gray matrix)	0.534085 ± 37	1.58688 ± 7		66 ± 3	1.3 ± 0.5	0.87 ± 0.35
Zag#3 (clast)	0.533983 ± 39	1.58664 ± 13		4 ± 1	<0.54	Not determined
NWA801 (bulk)	0.534239 ± 25	1.58704 ± 11	0.00955	20-30	3.7 ± 0.4	1.2 ± 0.4
Cook011 (bulk)	0.534088 ± 18	1.58690 ± 9	0.00699	9.5	1.5 ± 0.3	0.80 ± 0.37

Ψ values were calculated as follows; $$\Psi = \frac{(^{150}Sm/^{149}Sm)_{sample} - (^{150}Sm/^{149}Sm)_{STD1}}{(^{150}Sm/^{149}Sm)_{STD2} - (^{150}Sm/^{149}Sm)_{STD1}} \times \frac{\sigma_{STD2}}{\sigma_{sample}} \times (5.94 \times 10^{15})$$

where σ_{STD2}=5.0, σ_{sample}=5.7 for Kapoeta and 5.6 for Zag, NWA801, and Cook011 were used for the calculation.

$\varepsilon_{Sm}/\varepsilon_{Gd}$ values are defined as follows; $$\frac{\varepsilon_{Sm}}{\varepsilon_{Gd}} = \frac{\dfrac{(^{150}Sm/^{149}Sm)_{sample} - (^{150}Sm/^{149}Sm)_{STD}}{1 + (^{150}Sm/^{149}Sm)_{sample}}}{\dfrac{(^{158}Gd/^{157}Gd)_{sample} - (^{158}Gd/^{157}Gd)_{STD}}{1 + (^{158}Gd/^{157}Gd)_{sample}}}$$

Figure captions

Figure 1. Diagrams of (a) $^{149}Sm/^{152}Sm$ vs. $^{150}Sm/^{152}Sm$, and (b) $^{157}Gd/^{160}Gd$ vs. $^{158}Gd/^{160}Gd$ showing the isotopic shifts due to neutron capture reactions. STD in the figure means a terrestrial standard material without neutron irradiation (see text).

Figure 2. A correlation diagram between CRE age (Ma) and neutron fluence for each sample used in this study. The neutron fluences are estimated from the Sm isotopic shifts (Table 2). The CRE ages are from references. The error bars are calculated from the isotopic data with 2σ of mean.

Figure 3. A diagram of effective macroscopic cross section (Σ_{eff}) versus the balance of Sm and Gd isotopic shift ($\varepsilon_{Sm}/\varepsilon_{Gd}$) for extraterrestrial samples. A shaded zone represents thermalized neutron energy spectra based on LCH model (Lingenfelter et al., 1972). The data points for open symbols (aubrites, chondrites, and A-15, 16, 17) are from references (Hidaka et al., 1999, 2000, 2006; Hidaka and Yoneda, 2007). The data for closed symbols are in this study. The error bars are calculated from the isotopic data with 2σ of mean.

Figure 4. Chondrite-normalized REE patterns of chemical leachates from Kapoeta. Kapoeta #2 and #3 are acid-leachates from 2M HCl and aqua regia, respectively. Kapoeta #4 is acid residueobtained after the acid-leaching treatment (see text).

Fig. 1 Hidaka and Yoneda

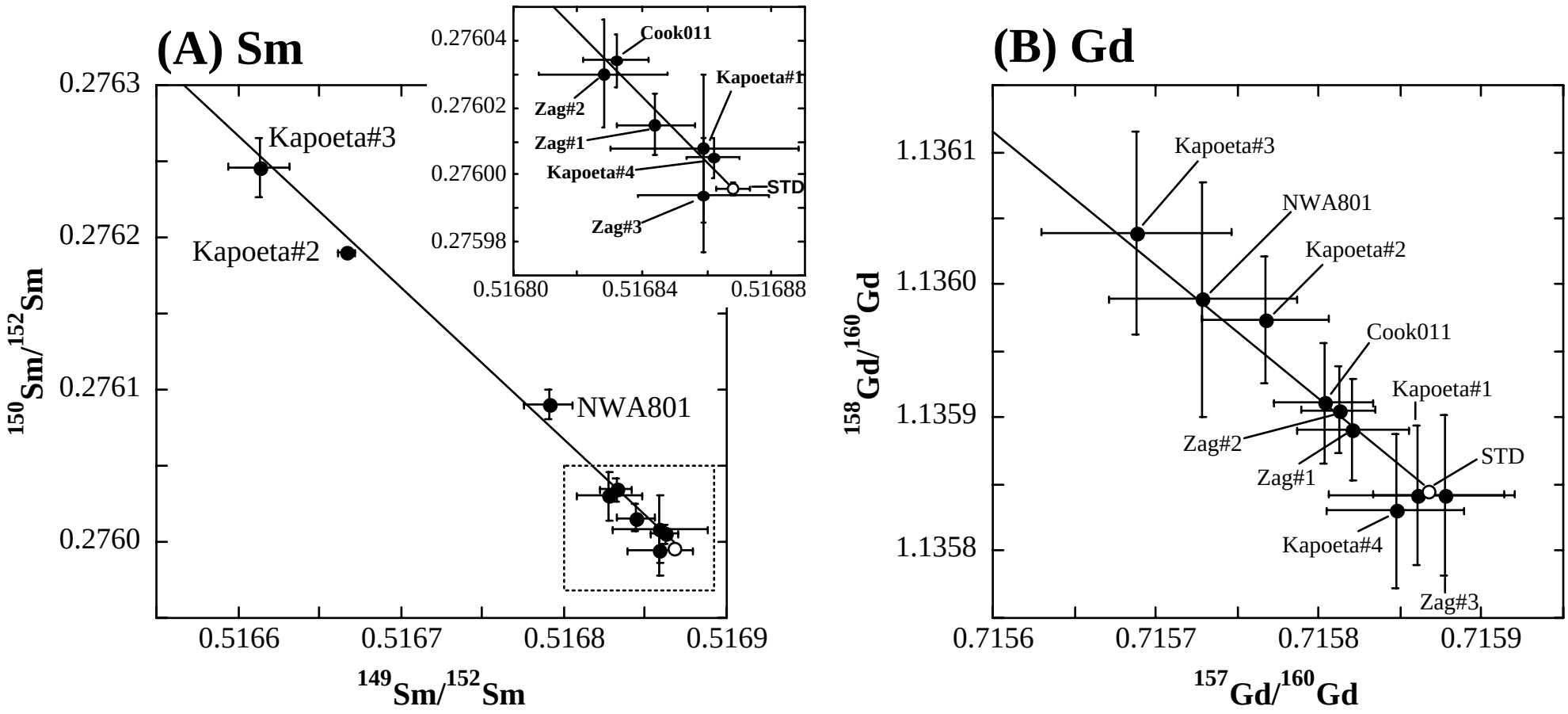

Fig. 2 Hidaka and Yoneda

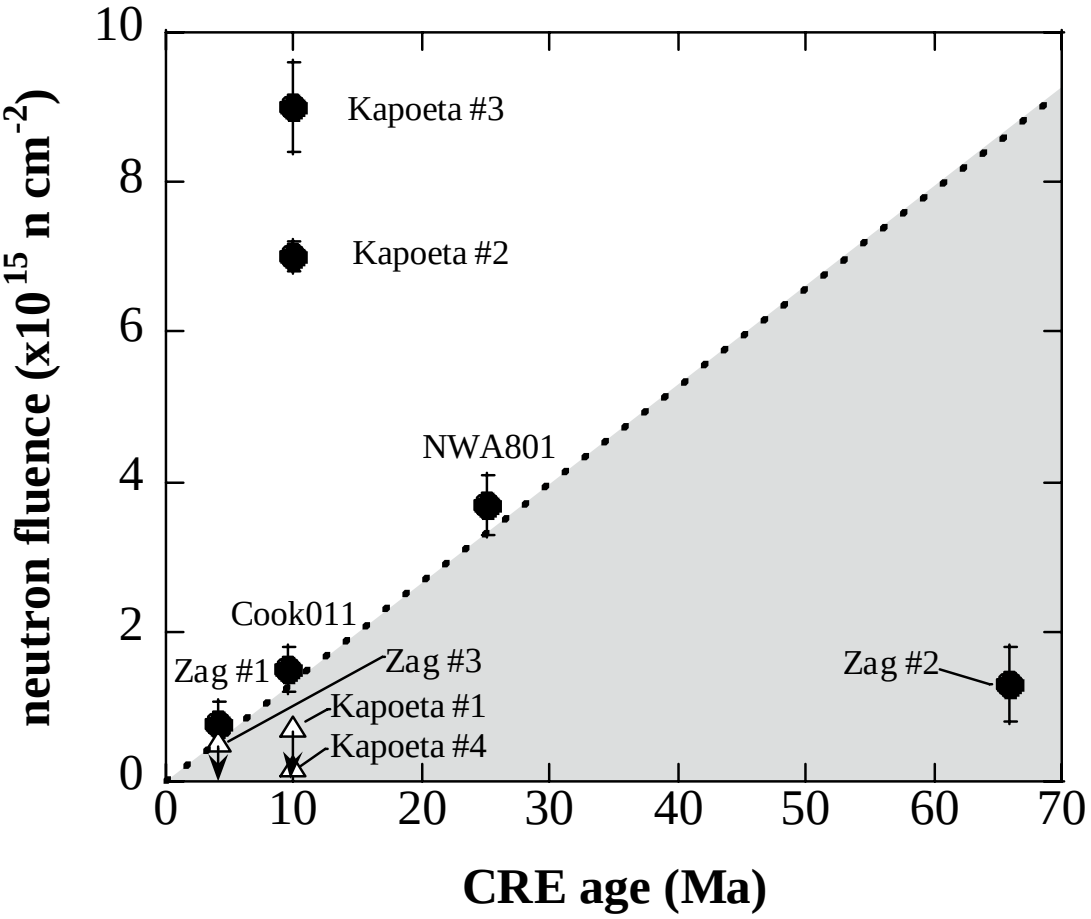

Fig. 3 Hidaka and Yoneda

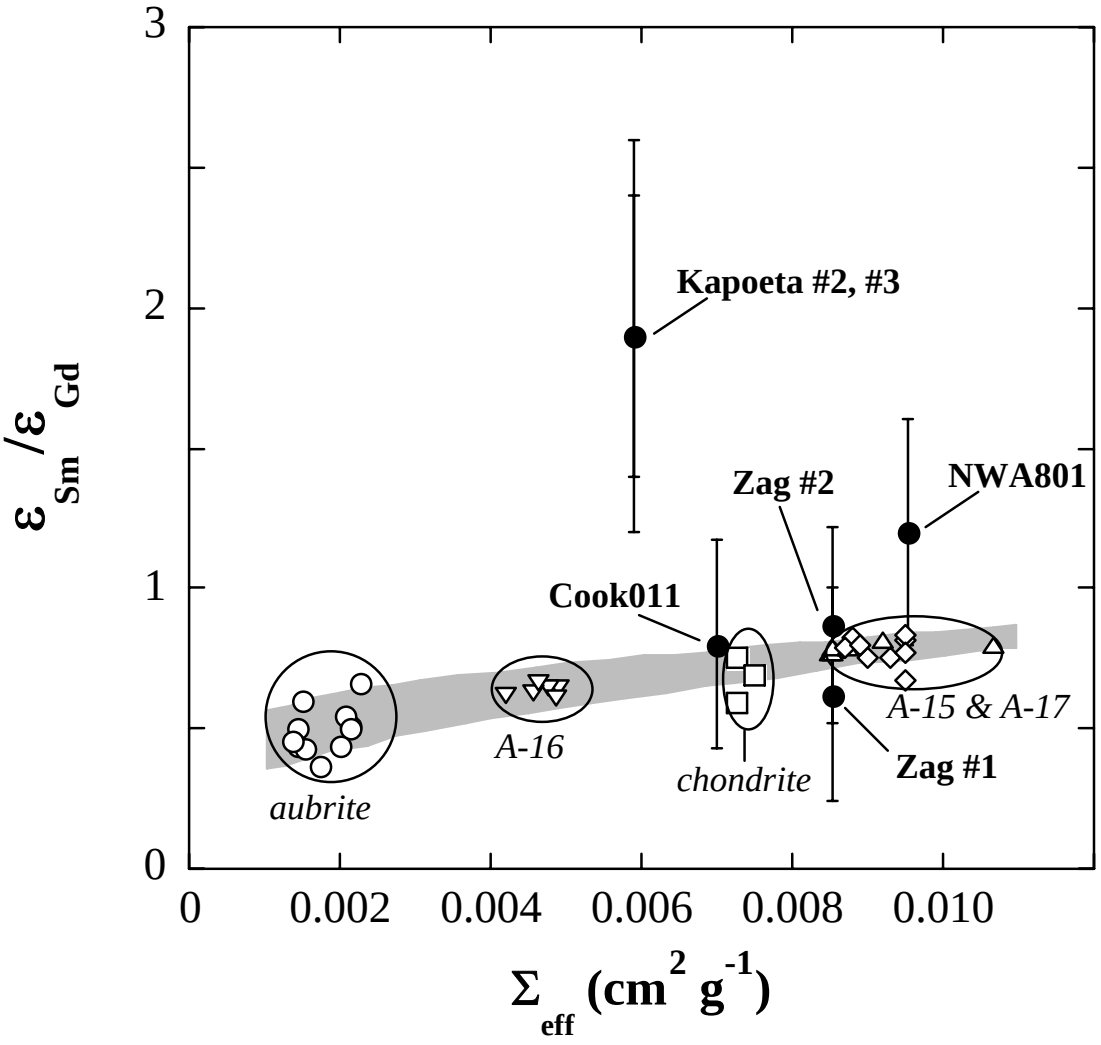

Fig. 4 Hidaka and Yoneda